DEVELOPMENT OF TISSUE-EQUIVALENT HEAT-SENSITIVE GEL FOR THE EXPERIMENTAL VERIFICATION OF NEAR INFRARED (NIR) LASER-MEDIATED CANCER DETECTION AND THERAPY

A Thesis
Presented to
The Academic Faculty

by

Arsalan K. Siddiqi

In Partial Fulfillment
of the Requirements for the Degree
Master of Science in the
George W. Woodruff School of Mechanical Engineering

Georgia Institute of Technology
August 2009

DEVELOPMENT OF TISSUE-EQUIVALENT HEAT-SENSITIVE GEL FOR THE EXPERIMENTAL VERIFICATION OF NEAR INFRARED (NIR) LASER-MEDIATED CANCER DETECTION AND THERAPY

Approved by:

Dr. Sang Hyun Cho, Advisor
School of Mechanical Engineering
Georgia Institute of Technology

Dr. C.-K. Chris Wang
School of Mechanical Engineering
Georgia Institute of Technology

Dr. Eric Elder
Department of Radiation Oncology
Emory University School of Medicine

Date Approved: April 28, 2009

ACKNOWLEDGEMENTS

There are many individuals who have made this work possible. I want to begin by thanking my advisor, Dr. Sang Cho, for his unwavering support and incessant words of encouragement and optimism. I am grateful for Dr. Cho's countless helpful suggestions and I feel very fortunate to have had the privilege to learn from him and have him as a mentor. Next, I would like to thank my parents for their support and enthusiasm, and for instilling in me the value of education and hard work.

I would also like to thank my committee members, Drs. Chris Wang and Eric Elder, for providing valuable suggestions. I want to extend my thanks to Dr. Johannes Leisen for training and giving me access to small animal magnetic resonance imaging machine at Georgia Tech. I am grateful to members of our research group, Dr. Seong-Kyun Cheong, Bernard "Tripp" Jones, and all undergraduate students for helping me in completing this work. Finally, I would like to thank U.S. Department of Defense, Breast Cancer Research Program, Concept Award, W81XWH-08-1-0686, for supporting this work.

TABLE OF CONTENTS

LIST OF TABLES

LIST OF FIGURES

SUMMARY

Polymer gels have long been used in clinics and laboratories to obtain three dimensional dose profiles in radiation therapy. Recent advances and emergence of thermal imaging and therapy modalities have again prompted the use of tissue equivalent heat-sensitive gels for phantom measurements and treatment verification purposes. Much effort has been made in developing tissue equivalent phantom materials to accurately predict and capture the extent of heat evolution and thermal damage. In order for any heat-sensitive gel to be feasible and clinically acceptable, it must meet the following requirements: tissue equivalency in thermal and optical properties, thermal stability at high temperatures, and capability of capturing the heat damage three dimensionally. Additionally, an ideal thermal phantom material must be reproducible, inexpensive, and easy to fabricate. The existing thermal gels either use extremely toxic chemicals or do not completely satisfy the aforementioned requirements. Thus, the primary motivation for this research was to develop a tissue equivalent phantom made of relatively nontoxic substances that has high thermal stability and that has the ability to capture thermal damage across volume.

Two agar based non-toxic thermal gels, TG1 and TG2, have been developed and characterized in terms of their optical response to 808 nm Near Infrared (NIR) laser and thermal damage. Magnetic resonance imaging was used to image the gels and quantify thermal damage based on T2 values. TG1 gel, agar and bovine serum albumin (BSA) mixture, was found not to be optically tissue-equivalent compared to the previously reported gelatin based gel phantom [5]. However, TG1 gel has demonstrated unambiguous digital response capable of distinguishing temperature of at least 70 °C compared to the sample receiving no heat. Additionally, focusing only in the thermal therapy temperature regime (60 – 80 °C), TG1 gel produced high degree of linearity (R^2 = 0.9935). This linearity and predictable response give TG1 gel a potential to be used as

thermal dosimeter in thermal therapy applications. On the other hand, TG2 gel containing agar mixed with BSA and Intralipid has exhibited tissue equivalency based on laser transmission measurements with 808 nm NIR laser. According to the current results, it is evident that TG2 gel is less sensitive to heat than TG1 gel. TG2 gel can exhibit the heat damage based on T2 values, only when the temperature reaches 80 °C. This digital response is considered less sensitive in view of the fact that BSA starts to undergo denaturing and cause optical density change at approximately 70 °C. Both gels, however, have shown to be thermally stable at temperatures up to 80 °C with no evidence of gel melting being observed. The gels can be easily prepared with basic laboratory equipment, making them viable for clinical environment. Additionally, the ability of these gels to be quickly scanned under MRI is an attractive incentive for clinical applications.

CHAPTER 1

INTRODUCTION

Radiation has long been used to image and to treat variety of diseases, especially cancers. Cancer accounts for 1 of every 4 deaths and is the second leading cause of death in the United States [1]. Nearly 1.4 million new cancer cases were diagnosed in 2008 [1]. Early diagnosis and improved treatment methods have shown to improve overall survival rates [1]. In recent years, thermal imaging and thermal therapies involving hyperthermia have emerged as viable alternative to radiation (i.e., ionizing radiation) [2]. Whether it is radiation or hyperthermia, polymer gels have been used in clinics and laboratories for both quality assurance and treatment verification purposes and for experimental testing of new treatments and diagnostic modalities.

Radiation therapy involves using ionizing radiation to target and destroy cancerous cells while sparing healthy and critical structures. From the delivery standpoint, it is important to know precisely where and how much radiation was delivered. There are many detectors and devices available that give two-dimensional (2D) dose information. However, there are very few methods to obtain three dimensional (3D) dose profiles reliably. One way to obtain 3D dose over a volume is to use radiosensitive gels. Radiosensitive gels can be manufactured easily in a standard laboratory setting without any complicated equipment or techniques. Once made, they can be poured into any mold or container and allowed to solidify. Once solidified, they can be irradiated with ionizing radiation such as X-rays, gamma rays, etc. which induces an optical property change in the gels [3]. The gel can be read using an optical computed tomography (CT) or magnetic resonance imaging (MRI). One of the most widely used radiosensitive normoxic polymer gel is Methacrylic and Ascorbic acid in Gelatin Initiated by Copper (MAGIC). In MAGIC gel, the spin relaxation rate, R2, is proportional to absorbed dose, producing linear dose versus relaxation rate in the range of 0-30 Gy [3].

Similar to their use in radiation, gels have also been used to verify delivery of thermal therapy modalities [2]. Thermal therapy typically involves shining a laser (or equivalent light source) to raise the temperature high enough to destroy diseased tissue. Thus, it is important for thermal gel to exhibit optical and thermal properties similar to that of tissue to accurately predict heat generation and damage. Tissue equivalent thermal gel phantoms based on polyacrylamide and gelatin have previously been developed and well characterized [2,4,5]. In order for any heat sensitive gel to be feasible and clinically acceptable, it must have similar thermal and optical properties as those of tissue, be thermally stable at high temperatures, and it must be able to capture the resulting heat damage to allow for comparison between computational predictions and experimental measurements [2].

McDonald et al. have developed a heat sensitive gel based on acrylamide that exhibits optical properties similar to that of tissue and it is able to withstand temperatures up to 80 °C and capture the heat damage three dimensionally [2]. However, acrylamide is a severe neurotoxin and it is a tremendous hazard for all personnel especially in a clinical setting. Chen et al. have attempted to develop tissue equivalent phantom using nontoxic substances that has optical properties matching those of tissue but it cannot withstand temperatures above 25 °C nor can it permanently capture any thermal damage [5]. Thus, the primary motivation for this research is to develop a tissue equivalent phantom made of relatively nontoxic substances that has high thermal stability and that has the ability to capture thermal damage across volume.

This research will develop and characterize two different agar based thermal gels using nontoxic substances that may be used for both diagnostic and therapeutic applications. Optical transmission measurements will be made to determine tissue equivalency for each gel type and compared to previously reported tissue equivalent gel. Thermal characterization will be carried out to establish each gel's thermal stability and heat sensitivity.

CHAPTER 2

BACKGROUND

In recent years, various applications based on a physical phenomenon known as photothermal effect have been developed, especially in connection with the use of optically-tunable metal nanoparticles that emit intense heat to the surrounding medium as a result of strong absorption of light at their plasmon resonance frequency. This section will provide an overview of photothermal effect and how it can be used in thermal therapy and diagnosis for various diseases including cancer. Additionally, an overview of existing heat sensitive gel recipes will be presented along with the role of MRI in gel dosimetry and thermometry.

2.1 Photothermal Effect in Diagnosis and Therapy

When electromagnetic radiation interacts with matter, several events are possible. It can result in absorption, emission, and or scattering of radiation [6]. The absorption of an incident electromagnetic radiation leads to production of heat by several nonradiative processes resulting in noticeable changes in temperature, pressure, and refractive index of the medium [6]. This is traditionally known as photothermal effect. In 1964, after the invention of laser, Gordon et al. noticed beam divergence from liquid samples which were located in path of gas laser cavity, and it was later that this phenomenon was understood in terms of "thermal lens" effect due to heat induced by Gaussian laser beam [6]. Photothermal interrogative methods allow for thermal emission to be detected by photothermal radiometry, and reflectivity/absorptivity changes are measured with thermal reflectance, transient piezo-reflectance, and transmission measurements.

One of the advantages of photothermal investigation is that this technique is highly sensitive and extends itself to broad range of materials (irrespective of phase) and appearance (transparent/opaque), or shape. It works with any type of radiation including

radiofrequency, visible light, microwave, ultraviolet (UV), and especially infrared (IR) [6]. NIR laser mediated cancer detection and therapy exploits one of the most attractive aspects of photothermal effect. Photothermal detection method is nondestructive and non-contact that can reveal optical and thermal properties over very small areas [6]. Such high spatial resolution has the potential to detect very small tumors using photothermal detection methods. Temporally, photothermal detection spans over seconds to femtoseconds, making it ideal for clinical applications.

Photoacoustic effect gives rise to change in medium's density and can be measured either acoustically or optically [6]. However, unlike photothermal effect, photoacoustic effect results in no heat production. Photoexcitation results in a pressure wave that is comprised of radiation pressure, electrostriction, thermoelastic expansion, photoinduced volume change, gas evolution, boiling, ablation, and dielectric background [6]. Similarly, refractive index changes in medium resulting from photoexcitation can be induced by the pressure wave, density change, temperature change, molecular alignment, vibrational excitation, rotational excitation, or concentration change [6]. Photo-optical effect is defined as modification of a medium's absorbance or refractive index as a consequence of photoexcitation [6]. Figure 2.1 summarizes the photothermal effect and its various outcomes. In condensed phases, the thermal energy liberated by radiationless transitions will be observed after photoexcitation by any means as long as resonance is matched. It is this premise on which many medical detection techniques operate to identify cancerous lesions/hotspots that have been tagged with absorbing dyes, nanoparticles, fluorescent markers, etc. Photothermal interrogation can be carried out on surfaces and interfaces, in addition to bulk phases, due to changes resulting in intensity, polarization, optical path, and reflection angle of the reflected optical radiation [6]. The reflection angle is sensitive to surface condition, which is a hallmark of photothermal effect [6].

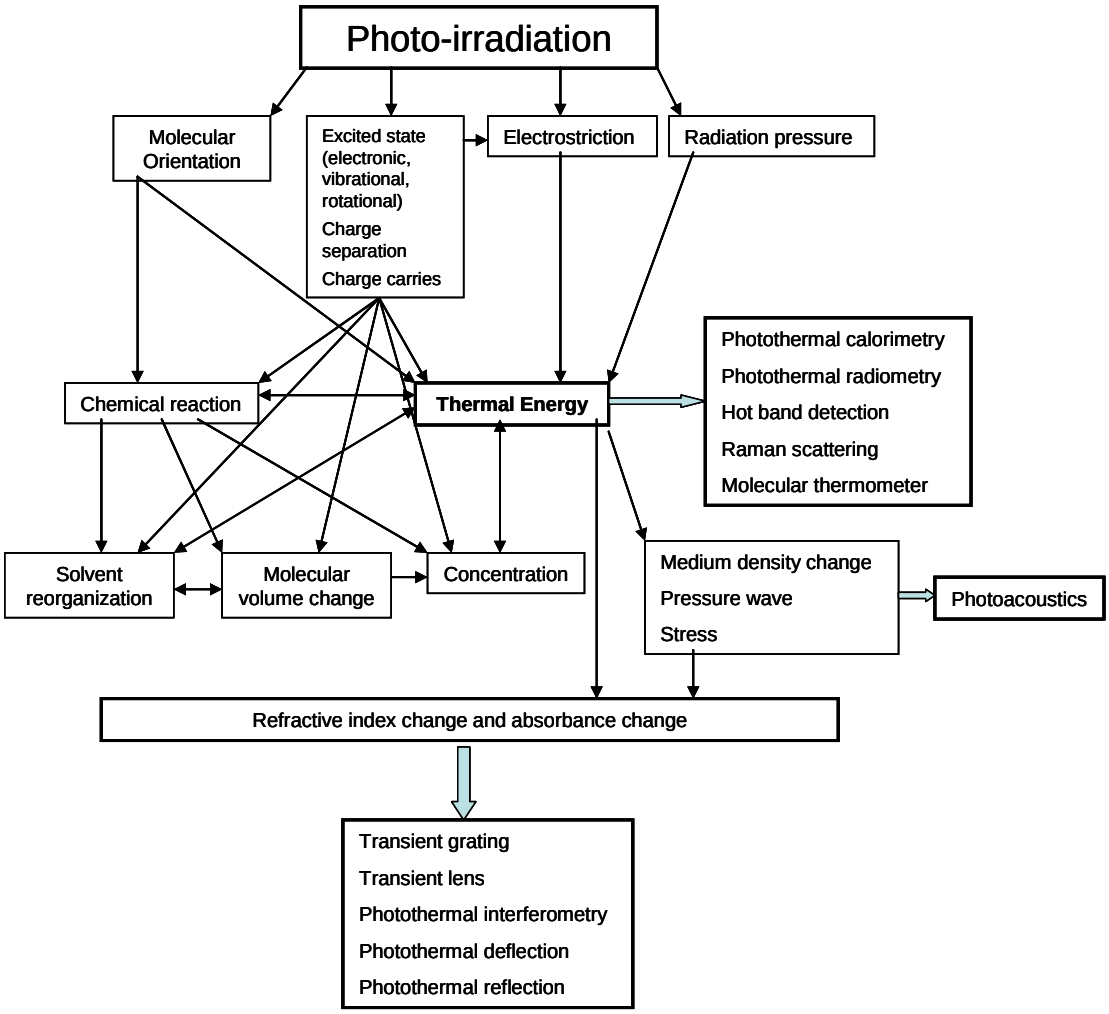

Figure 2.1: Photothermal effect and its outcomes resulting from photo-irradiation; arrows connect cause and effect. Figure adapted from [6].

In terms of therapy, photothermal effect has been used to raise temperature high enough to induce cell death in the diseased target tissue. One of the areas where nanotechnology has shown promising future is cancer therapy. Rapid temperature rise has been achieved when the target loaded with nanoparticles whose resonance frequency matches that of applied electromagnetic radiation, to further facilitate photothermal effect [7].

2.2 Thermal Therapy and Phantoms

Successful utilization of photothermal effect, discussed in previous section, has lead to the emergence of variety of thermal therapies. The primary objective of a thermal therapy is to increase the temperature of tissue beyond a threshold (usually 50-90 °C) to induce permanent tissue damage to achieve therapeutic benefit [8]. One of the advantages of thermal therapy is that it is relatively noninvasive and allows for rapid delivery and cell death [2]. As discussed earlier, heat can result from various sources such as lasers, ultrasound, microwaves, etc. Thus, the most critical and fundamental aspect of thermal therapy involves treatment planning. Much effort has been made in developing tissue equivalent phantom materials to accurately predict and capture the extent of heat evolution and thermal damage. In order for any heat sensitive gel to be feasible and clinically acceptable, it must meet the following requirements: tissue equivalency in thermal and optical properties, thermal stability at high temperatures, and capability of capturing the heat damage three dimensionally to allow for comparison between thermal therapy devices and quality assurance tasks [2]. Further, an ideal thermal phantom material must be reproducible, inexpensive, and easily fabricated [2]. Finally, the most ideal thermal phantom would satisfy all of the previously mentioned requirements and use relatively nontoxic substances so that phantom creation can be carried out in clinical setting without elaborate laboratory setup and safety precautions. The next several subsections will provide an overview of several existing thermal phantoms that have been developed and characterized.

2.2.1 Acrylamide Based Thermal Gels

Polyacrylamide based thermal gels are created by cross-linking acrylamide monomer with an initiator, usually *N,N'*-methylene-bis-acrylamide [2,4]. Polyacrylamide based thermal gels have high melting point which make them thermally stable in thermal

therapy temperature regimes. They have mechanical properties that resemble muscle tissue and transparent in the NIR [4]. McDonald et al. have developed a thermal gel phantom using acrylamide as base that exhibits thermal and optical properties similar to that of tissue and it has the ability to capture thermal damage over an entire volume [2]. Figure 2.2 is a schematic of thermal damage captured in McDonald et al.'s thermal phantom resulting from ultrasound probe heating.

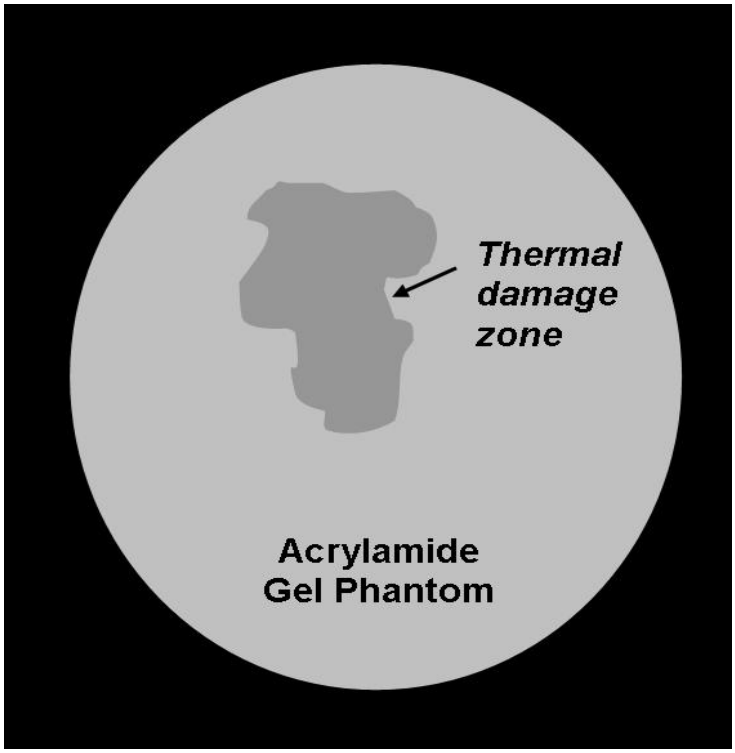

Figure 2.2: Schematic showing MRI slice of acrylamide thermal phantom where dark grey area represents the coagulated volume (thermal damage site). Figure adapted from [2].

Bovine serum albumin (BSA) is a heat-sensitive protein first used by Bouchard and Bronskill and later by McDonald et al. to capture heat damage shown in Figure 2.2 [2]. It is destruction of this heat-sensitive protein that is responsible for visualization of heat damage within the phantom [2]. Additionally, intralipid solution is frequently added to obtain acoustical and optical properties similar to that of tissue [2, 4, 5]. Intralipid solution is fat emulsion with milky white color making it an excellent scattering agent

[4]. However, the biggest drawback of acrylamide is its toxicity. Acrylamide is severe neurotoxin that requires extreme precautionary measures and poses a severe health hazard.

2.2.2 Albumen and Agar Based Phantoms

Another thermal phantom material that is often used to study laser illumination is albumen and agar system [4]. Albumen consists of approximately 10% globular proteins, 0.05% lipids, and 89% water [4]. Albumen powder, condensed form of egg white, is homogenous and exhibits thermal properties similar to tissue. Heating causes an irreversible visible damage, resulting in unfolding of albumen proteins that precipitate out and form aggregates. These aggregates are noticeably white in color, increasing the scattering coefficient [4]. Albumen powder dissolved in water makes an instant liquid thermal phantom, however most applications require tissue equivalent solid phantoms. Agar is used in conjunction with albumen to act as solidifying agent and to add mechanical strength to create solid phantom [4]. However, agar and albumen are clear when dissolved in water, which make agar and albumen phantoms weakly absorbing to NIR electromagnetic radiation [4]. Additionally, tissue equivalency cannot be claimed with such response to NIR light. Consequently, thermal phantoms have been developed with agar, albumen powder, and incorporation of absorbing dye such as Naphthol Green (effective in NIR wavelengths) as a viable relatively nontoxic optical phantom [4]. Experimental measurements indicate that this phantom system has μ_s' (reduced scattering coefficient) and μ_a (absorption coefficient) values of 2.7 ± 0.1 cm^{-1} and 0.5 ± 0.1 cm^{-1}, respectively, in native state while μ_s' = 13.1 ± 0.5 cm^{-1} and μ_a = 0.7 ± 0.1 cm^{-1} in coagulated state, which are typical of soft tissue in NIR [8].

2.2.3 Gelatin Based Optical Phantoms

Gelatin based phantoms are typically used to measure thermal reactions, or slight temperature increases, and in detection applications for real-time MRI thermometry involving laser phototherapy [5]. The phantom primarily consists of gelatin dissolved in water and liposyn (fat suspension) to match optical properties with biological fatty tissue such as breast [5]. Disadvantages of gelatin phantom are its low melting temperature and inability to capture heat damage. Gelatin melts at approximately 30 °C which makes it an impractical phantom for thermal therapy temperature regimes (50-80 °C). Additionally, gelatin based thermal phantoms do not possess the same mechanical strength that acrylamide or agar/albumen phantoms do in order to resemble biological tissue.

2.2.4 Agar and Intralipid Based Phantoms

Tissue equivalent phantoms are relevant for variety of medical applications especially optical mammography for cancer diagnosis and detection [9]. Cubeddu et al. have developed a solid tissue equivalent phantom to be used for photon migration studies using agar, Intralipid, and black ink [9]. Agar acts as a solidifying agent and gives mechanical strength, black ink serves as an absorbing medium, and Intralipid as scattering agent. Agar gel alone is insufficient for photon migration studies since it has negligible absorbance and low turbidity [9]. Optical parameters were determined using time-resolved transmittance measurement. This phantom system showed μ_s' (reduced scattering coefficient) and μ_a (absorption coefficient) to vary linearly with Intralipid and ink concentrations, respectively [9]. With respect to agar content, a systematic decrease in μ_s' was observed. [9]. While this phantom system has shown tissue-equivalency, it cannot be used for thermal therapy applications due its inability to reveal any heat damage information.

2.2.5 Wax Based Phantoms

Wax is another common material used to make optical phantoms. Cancerous changes in tissue lead to change in refractive index and optical scattering [10]. Thus, it is not surprising that optical imaging modalities are emerging to exploit this change in refractive index and scattering to detect cancers in their earliest possible stages. Tissue equivalent optical phantoms made of paraffin wax and food coloring have been successfully made to study photon transport [10]. Various combinations of food colorings were used to match scattering profiles to specific tissues such as lungs, liver, spleen, muscle, etc. [10]. While tissue equivalency can be established using these non-toxic ingredients, however, such a phantom lacks the heat-sensitivity required for thermal therapy.

2.3 MRI in Gel Dosimetry

Magnetic resonance imaging (MRI) or simply (MR) was first used in gel dosimetry to investigate changes in irradiated Fricke dosimeter solutions and gels to obtain three dimensional dose distributions [3]. The signal in MRI is acquired from the hydrogen atom nuclei that consist of 1 proton and 1 electron orbiting the nucleus [11]. The positively charged proton has mass and an associated spin, giving the proton its angular momentum and magnetic moment. Consequently, external magnetic fields and electromagnetic waves have an influence on the proton, especially when the proton moves, creating voltage in receiver coil. When an external magnetic field is applied, the magnetic moments, or spins, are forced to align with the field and experience precession [11]. Precession of each nucleus is observed at specific speed called the *Larmor frequency* that is directly proportional to the applied magnetic field [11]. Larmor frequency indicates how the spins wobble in a particular magnetic field [11].

As the spins relax, longitudinal magnetization (z-direction), M_z, continues to increase due to the summation of individual magnetic vectors [11]. MRI machines have

magnets capable of producing strong magnetic fields, which result in stronger longitudinal magnetization [11]. A radiofrequency (RF) pulse is applied to rotate the longitudinal magnetization into transverse plane (xy-plane) by exactly 90°. An alternating voltage, corresponding to the Larmor frequency in a receiver coil, is induced due to the rotation of transverse magnetization around the z-axis [11]. This voltage signal is collected and processed to generate an image. Figure 2.3 shows how the nuclei are aligned in the presence of magnetic field and the role of RF pulse in MRI.

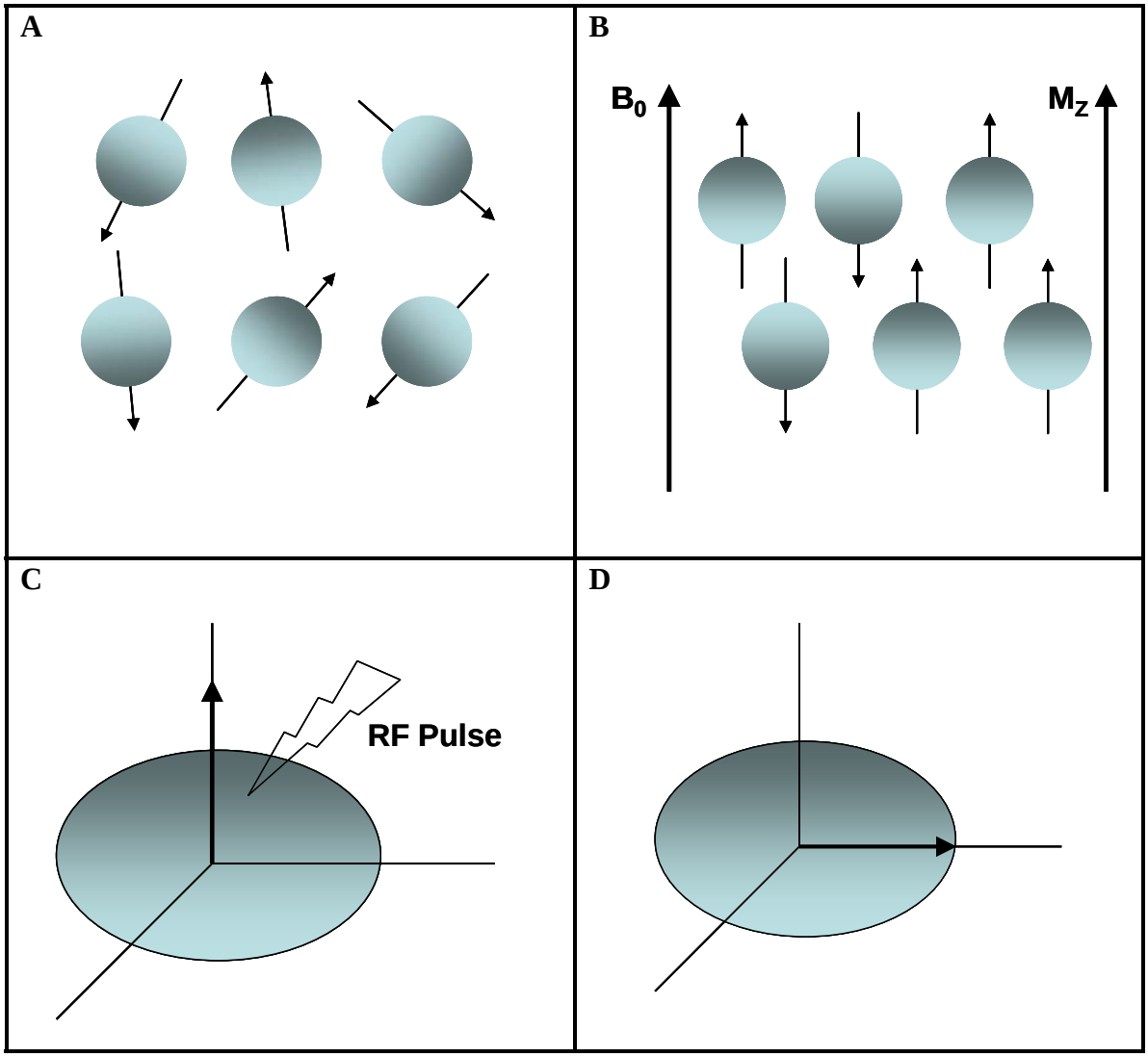

Figure 2.3: (a) When no external magnetic field is present, spins rotate in random direction. (b) When an external magnetic field, B_0, is applied, spins align with the field creating longitudinal magnetization, M_z. (c) RF pulse is applied to rotate the longitudinal magnetization by exactly 90° into transverse magnetization (d). Figure adapted from [11].

The transverse magnetization causes a very short-lived signal that fades quickly due to spins returning to stable states by processes called spin-lattice interaction (T1 relaxation) or spin-spin interaction (T2 relaxation) [11]. T1 relaxation or recovery refers to restoration of longitudinal magnetization, M_z, as transverse magnetization decays. T1 is the time constant for the recovery that depends on applied magnetic field and Brownian motion of molecules [11]. Spin-spin interaction or T2 relaxation is essentially the decay of transverse magnetization which occurs when phase coherence is lost causing some spins to become out of sync on their precessional paths [12]. Phase coherence is defined as the state when excitation causes part of the spins to precess synchronously with no separation in their circular paths [11]. Individual magnetization vectors begin to cancel each other, resulting in smaller transverse magnetization, and consequently weaker MR signal. It is important to remember that T1 and T2 relaxations occur simultaneously and are completely independent of each other. T2 relaxation is responsible for signal decrease within first 100-300 msec, while T1 relaxation occurs much later (0.5-5 sec) [11].

The contrast in MRI is determined by several factors including proton density, T1 time, and T2 time [11]. Emphasizing one of these parameters over others results in an image being weighted towards that particular parameter. Proton density refers to the number of excitable spins available per unit volume, controlling the maximum signal that can be obtained [11]. As previously described, T1 time is the time necessary for excited spins to recover and become available for subsequent excitation, while T2 time determines how fast the signal fades after excitation [11]. Having a large T1 time in conjunction with small T2 time or vice versa allows for high contrast especially for soft tissues. Another important parameter to consider is repetition time (TR). TR is the time between two successive excitations [12]. Optimizing TR is crucial for T1 weighted images because when TR is long, more excited spins are able to rotate back in the z-plane which ultimately causes an increase in the longitudinal magnetization which leads to

stronger MR signal [12]. Images that are strongly T1 weighted have a short TR and vice versa. Echo time (TE) refers to the time between when excitation pulse is applied and when the signal from that pulse is collected [11]. Short TE results in images that have low T2 weighting since T2 relaxation has just initiated and very little MR signal has decayed [11]. Table 2.1 lists the qualitative relationship between TE, TR, and image contrast weightings. Typically, T1-weighted spin echo sequence has TR/TE ratio of 340/13 msec, while T2 weighted sequence is taken with TR/TE of 3500/120 msec. Table 2.2 lists the appearance of several tissue types under T1 and T2 weighted acquisition.

Table 2.1: Relationship between TR and TE for image contrast weightings [11].

	TR	**TE**
T1 – weighted	Short	Short
T2 – weighted	Long	Long
Proton density – weighted (intermediate – weighted)	Long	Short

Table 2.2: Appearance of select tissues based on T1 and T2 weightings [11].

Tissue	**T1 – weighted image**	**T2 – weighted image**
Fat	Bright	Bright
Aqueous liquid	Dark	Bright
Tumor	Dark	Bright
Inflammatory tissue	Dark	Bright
Muscle	Dark	Dark
Connective tissue	Dark	Dark
Hematoma, acute	Dark	Dark
Hematoma, subacute	Bright	Bright
Fibrous cartilage	Dark	Dark
Hyaline cartilage	Bright	Bright
Compact bone	Dark	Dark
Air	No signal	No signal

CHAPTER 3

METHODOLOGY

Two novel heat-sensitive gels have been proposed for use in NIR laser mediated cancer detection and therapy without using any toxic substances. This chapter will describe the fabrication and testing of these two agar based gels. Testing phase involves determination of tissue-equivalency using NIR 808 nm laser transmission measurements and quantification of heat-response to correlate temperature and thermal damage. The first gel is 1.5 wt% agar and 25 wt% BSA mixture which will be referred to from this point as Thermal Gel (TG) 1. The second gel being proposed, TG2, also contains agar, BSA, and an additional Intralipid.

3.1 Fabrication of TG1: Agar + BSA

In order to make agar based TG1, 1.5% by weight agar powder (Sigma A1296) is mixed with an appropriate amount of purified water (e.g. 100 mL water requires 1.52 g agar powder). The solution is continuously stirred while being heated gradually to 85-90 °C on a standard hot plate. Once heated, the solution is allowed to cool to 55 °C when 25 wt% BSA (Boval Comp. CF-0020) is added and mixed thoroughly. The albumen protein solution must be added when agar gel temperature is below 60 °C to avoid prematurely denaturing the albumen protein. The gel can be poured into any container or mold and it starts to solidify at approximately 45 °C.

3.2 Fabrication of TG2: Agar + BSA + Lipid

TG2 is a slight variation of TG1 with the main difference being addition of Intralipid, a fat suspension, to be used as scattering medium. In order to make 110 mL of agar based TG2, 2.0 wt% agar powder (Sigma A1296) is mixed with 90 mL of purified water (90 mL water requires 1.84 g agar powder). The solution is continuously stirred while being heated gradually to 85-90 °C. Once heated, the solution is allowed to cool to

55 °C when 25 wt% BSA (Boval Comp. CF-0020) is added to the solution. Next, 20 mL of Intralipid (20% emulsion, Sigma) is added and mixed completely. Note, agar concentration is increased slightly from TG1 to compensate for mechanical strength that is lost due to the addition of Intralipid.

3.3 Laser Transmission Measurements

Laser transmission measurements were made to determine tissue-equivalency of TG1 and TG2 and compared them with previously reported gelatin based tissue-equivalent gel by Chen et al. [5]. The gelatin based tissue-equivalent gel is created by mixing 2 g of gelatin powder (Type A 300 bloom, Sigma) in 80 mL of purified water and heating to 45 °C to completely melt the gelatin, when 20 mL of 20% Intralipid solution is added [5]. Figure 3.1 shows the appearance of three gels after they have solidified.

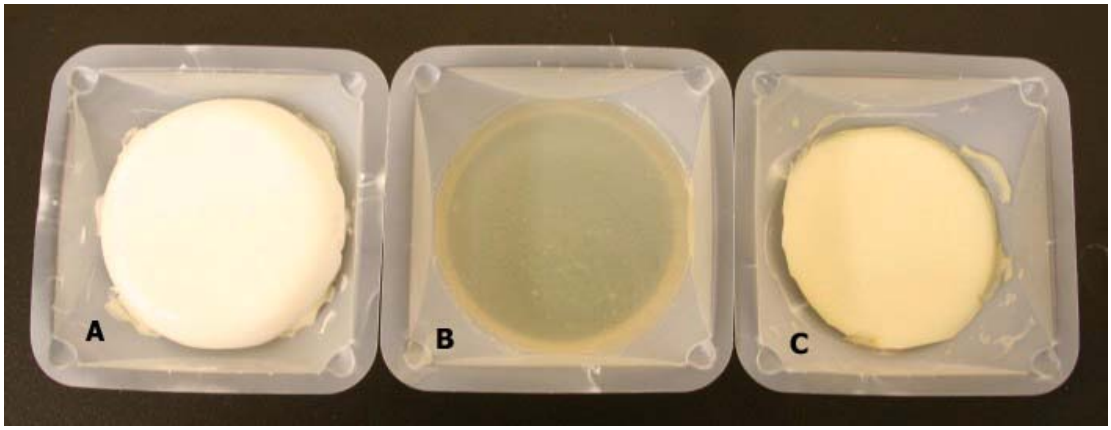

Figure 3.1: Physical appearance of (A) gelatin based tissue-equivalent gel created by Chen et al, (B) TG1: 1.5 wt% agar mixed with BSA, (C) TG2: 2 wt% agar mixed with BSA and Intralipid.

For optical transmission measurements, an 808 nm NIR laser (PLT-808-150-1000-BF, PLT Technology, Inc.) was used for illumination. The laser was operated at maximum current (1880 mA) to produce 1 W. The gels were poured into cylindrical mold to create uniform and reproducible geometry for optical measurements. Figure 3.2

shows the mold used to make cylindrical gel phantoms with 2.7 cm diameter and 2.3 cm height.

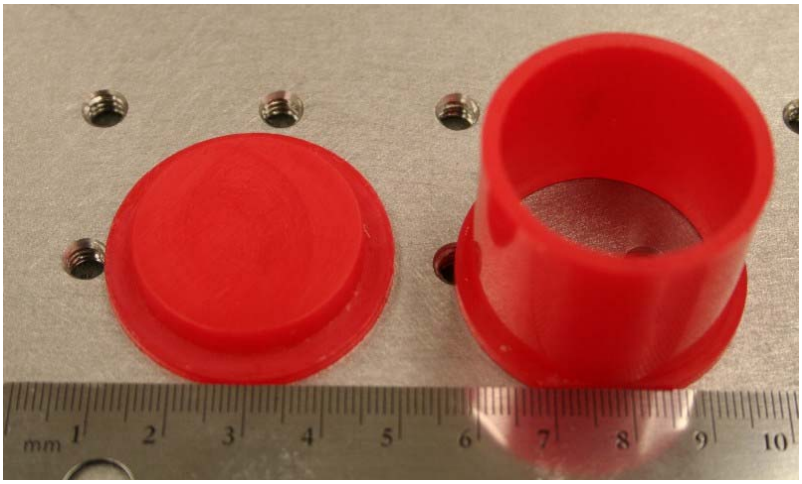

Figure 3.2: Cylindrical mold used to cast gels for laser transmission measurements.

A silicon photodiode detector/amplifier with an operational amplifier and feedback resistor and capacitor (SD 112-43-11-221, Advanced Photonix, Inc.) was used to collect laser transmission signal and voltage reading was obtained for each gel. This detector was chosen because of its relatively high sensitivity (≥ 80%) in NIR region (800-900 nm). The detector was operated by 5 V DC and has an active area of 2.54 mm x 2.18 mm. Figure 3.3 shows the photodiode detector as a metal can package and after it has been fitted to casing.

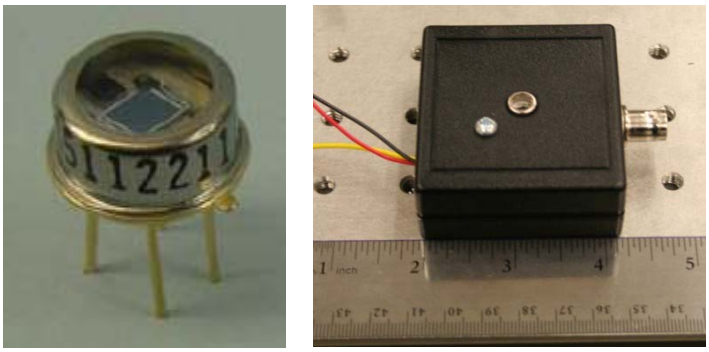

A **B**

Figure 3.3: (A) Silicon photodiode detector used to collect laser signal [13]. (B) Detector after it has been cased with wires coming out for power supply and BNC output connection.

Tissue equivalency was determined by laser transmission measurements in which silicon photodiode captured the voltage drop across each cylindrical gel phantom (2.3 cm height). The 808 nm laser and detector were aligned and cylindrical gel phantoms were placed in between laser and detector such that the laser was shone perpendicularly at the surface of phantoms. The detector was placed directly below the gel phantom to capture the laser transmission signal. The distance between the tip of the laser optical fiber and surface of the detector was 2.5 cm. A voltmeter was connected directly to the detector via BNC connection to display the voltage drop. The laser was operated at maximum current (1880 mA) to produce 1 W and illumination time was 20 seconds, until the voltage reading stabilized. The transmission measurements were made in the dark to avoid signal interference from ambient room lights. Figure 3.4 shows the experimental setup used for these transmission measurements.

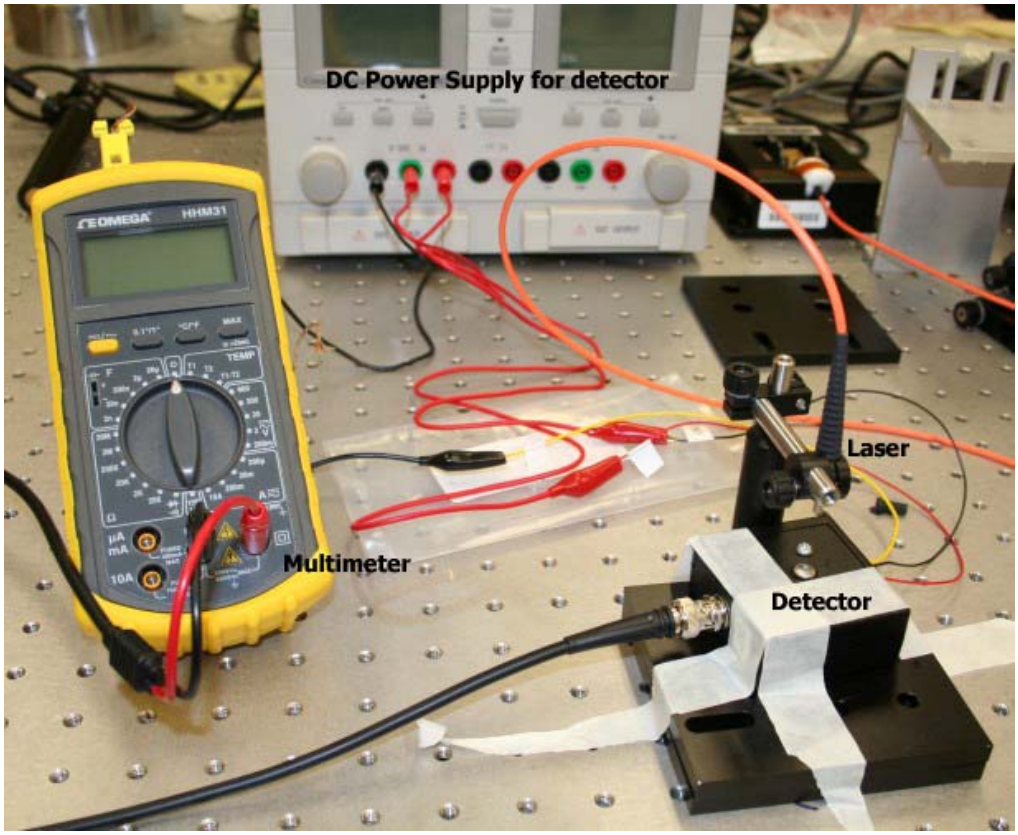

Figure 3.4: Experimental setup used for transmission measurements to determine tissue equivalency for each gel phantom.

3.4 Thermal Response and Heat Sensitivity of Agar Gels

In addition to tissue-equivalency in terms of their optical properties, the proposed agar based phantoms were characterized for their heat sensitivity and thermal response. The gels, both TG1 and TG2, were made according to recipes described in previous section. Once made, they were poured into clear plastic containers (2.4 cm diameter, 5 cm height) and allowed to set. Five samples were made for each gel type, with one serving as control. The gels were heated in a water bath to temperatures corresponding to thermal therapy regimes, 65-80 °C in 5 degree increments. A 6 inch hypodermic thermocouple needle probe with 1.5 mm diameter (HYP-3, Omega Eng.) was used to monitor the gel temperature. The gels were heated to target temperature (±1 °C) and held for 2 minutes before being removed. Once heated, the gels were allowed to return to room temperature before being scanned in MRI.

As shown in Figure 3.5, the gels were scanned in small animal MRI machine, Bruker 7T Pharmascan, with a maximum gradient strength 300 of mT/m. Five slices were obtained for each gel sample corresponding to the middle of the container. The gels were scanned using multi-slice multi-spin-echo sequence collecting 16 echo images for each slice. For TG1, agar and BSA gel, an echo time (TE) of 25.0 ms, and repetition time (TR) of 2070 ms were used. For TG2, agar containing Intralipid and BSA, TE = 12 ms and TR = 1000 were used to improve contrast. All gel images had 256 x 256 matrix, 3.0 cm field of view (FOV), 2.0 mm interslice distance, and 1.0 mm slice thickness. A region of interest (ROI) was defined, 0.5 cm^2, corresponding to the middle of the container, where average T2 value was obtained to quantify the damage resulting from heating.

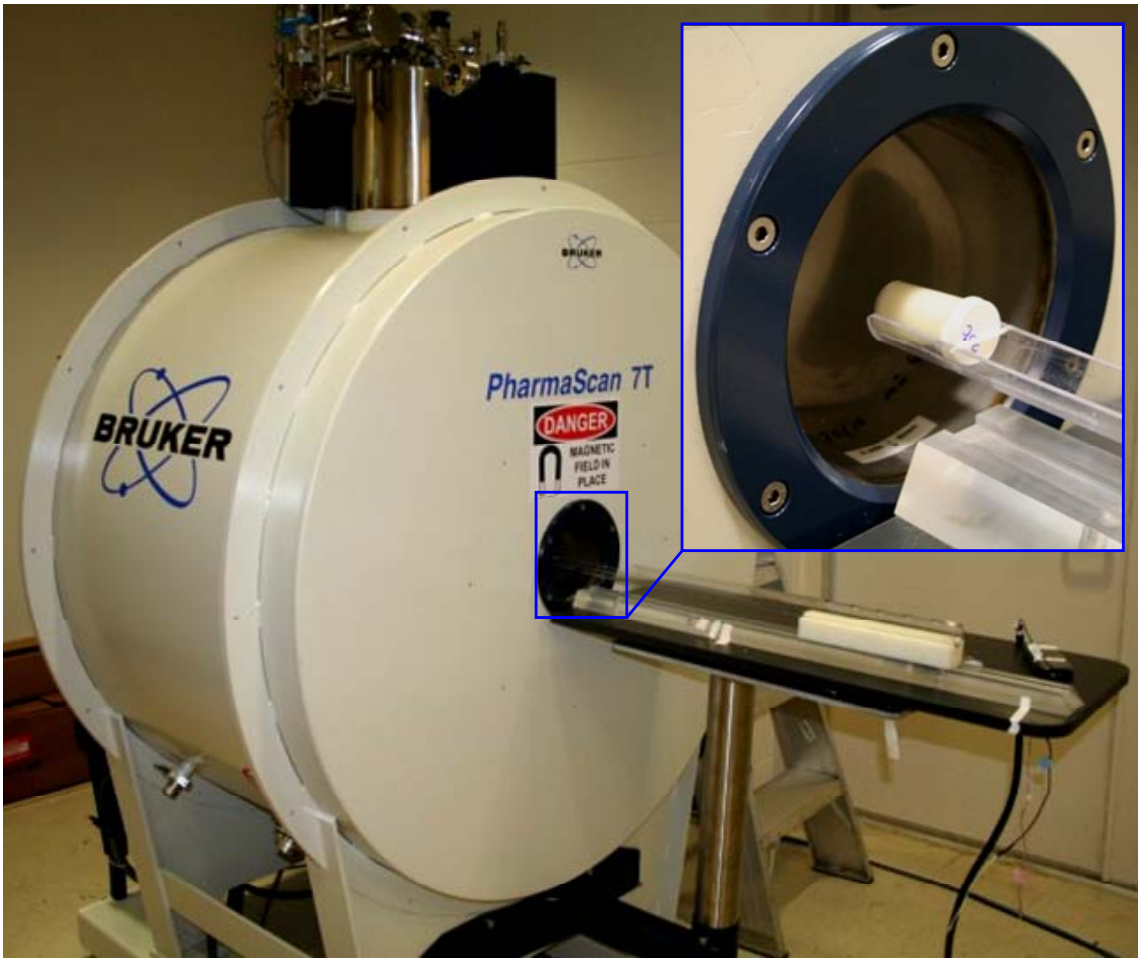

Figure 3.5: MRI setup used for scanning the gels.

CHAPTER 4

RESULTS

4.1 Laser Transmission Measurements

Laser transmission measurements were made to determine tissue-equivalency of two proposed gels, TG1 and TG2, compared to the previously reported tissue-equivalent gelatin and lipid gel by Chen et al [5]. Table 4.1 lists the voltage drop measured by the silicon photodiode detector in response to 808 nm laser illumination across 2.3 cm high cylindrical gel phantoms. A measurement was made without any gel in between laser and detector to establish a baseline for comparison purposes.

Table 4.1: Laser transmission measurements for each gel type.

Sample	Reading (V)
No Gel Phantom	-1.301
TG1: Agar + BSA	-1.310
TG2: Agar + BSA + Intralipid	-0.121
Gelatin Lipid Gel (Chen at al.)	-0.111

As shown in Table 4.1, TG1 shows negligible absorbance and low turbidity, making it optically equivalent to having no gel present. However, addition of Intralipid in TG2 has profound effect on optical property of the gel. In comparison with tissue equivalent gelatin gel, TG2 is considered optically tissue-equivalent for 808 nm laser illumination. The results agree with visual examination since Chen et al.'s gelatin and lipid phantom is milky white in color and TG2 has similar appearance shown in Figure 3.1. On the other hand, TG1 is relatively clear with no scattering media. Intralipid is an essential component in these gels because of its function as scattering media in establishing tissue equivalency. It is important to note that while laser transmission

method of optically characterizing the gels does not yield specific quantities of μ_s' (reduced scattering coefficient) and μ_a (absorption coefficient), however, the obtained values essentially give an effective attenuation coefficient (μ_{eff}) taking into consideration both absorption and scattering [4].

4.2 Thermal Characterization of TG1 and TG2

The gels were heated in a water bath to temperatures corresponding to thermal therapy regimes, 65-80 °C in 5 degree increments. The gels were heated to target temperature (±1 °C) and held for 2 minutes before being removed. For TG1, agar and BSA gel, there is a noticeable clear visual change in appearance with increasing temperature, as shown in Figure 4.1. The TG1 gel becomes increasingly opaque relative to the control sample resulting from destruction of BSA.

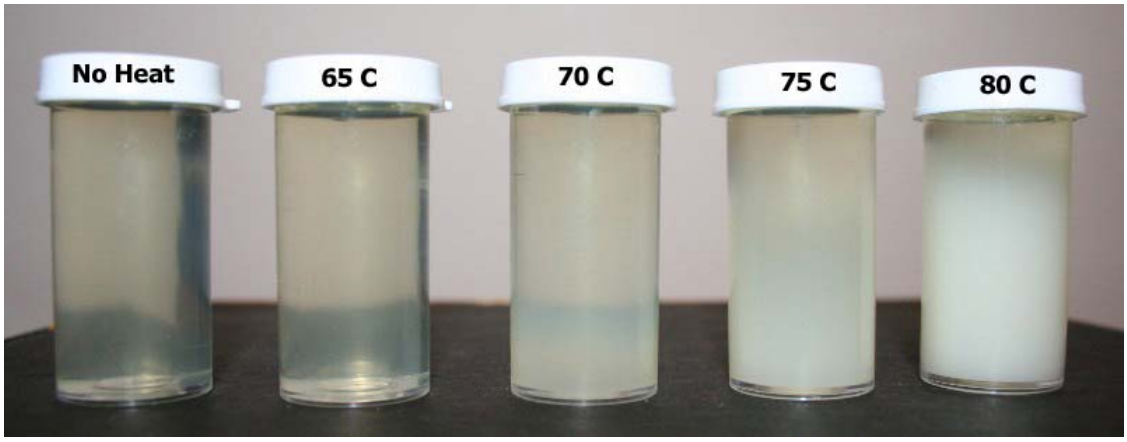

Figure 4.1: Physical change in appearance of TG1 gel in response to increasing temperature.

Thermal response and heat sensitivity was quantified in terms of gel's T2 values after scanning in MRI. Average T2 values were obtained from the central axial slice corresponding to the middle of the container. Figure 4.2 shows the MRI images of TG1 gels from central slice.

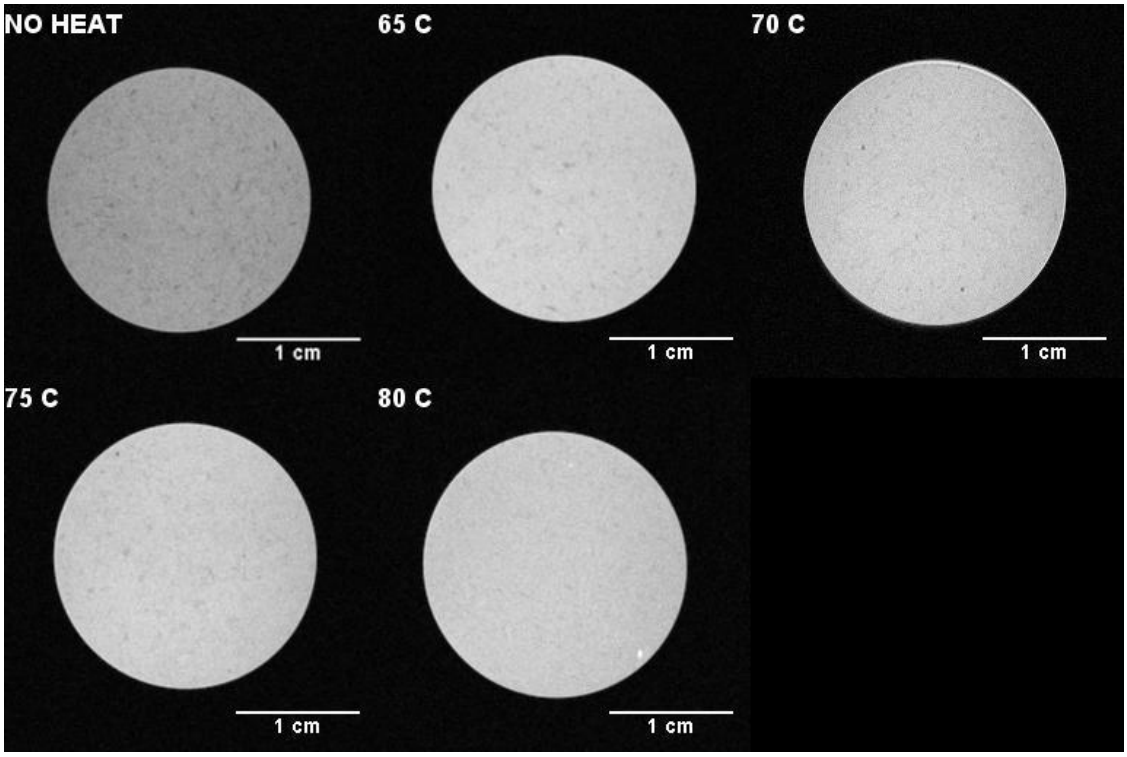

Figure 4.2: MRI images of TG1 gel samples.

Based on Figure 4.2, there is a noticeable difference in contrast from the control sample (no heat) to that of other samples, but there is negligible visual difference between each of the heated samples. Table 4.2 lists the average T2 values measured for each of the five TG1samples and their corresponding uncertainty to establish quantitative relationship. The average uncertainty in T2 values for all five samples is 5.03%.

Table 4.2: T2 values measured for TG1 gels as a function of temperature.

	T2 (msec)	**Error (%)**
No Heat		
(22 ± 1 °C)	74.419	4.61
65 ± 1 °C	71.319	4.41
70 ± 1 °C	67.558	5.12
75 ± 1 °C	63.667	5.08
80 ± 1 °C	59.447	5.93

The T2 relaxation rate, R2 (R2 = 1/T2), is also plotted as a function of temperature, shown in Figure 4.3 for TG1.

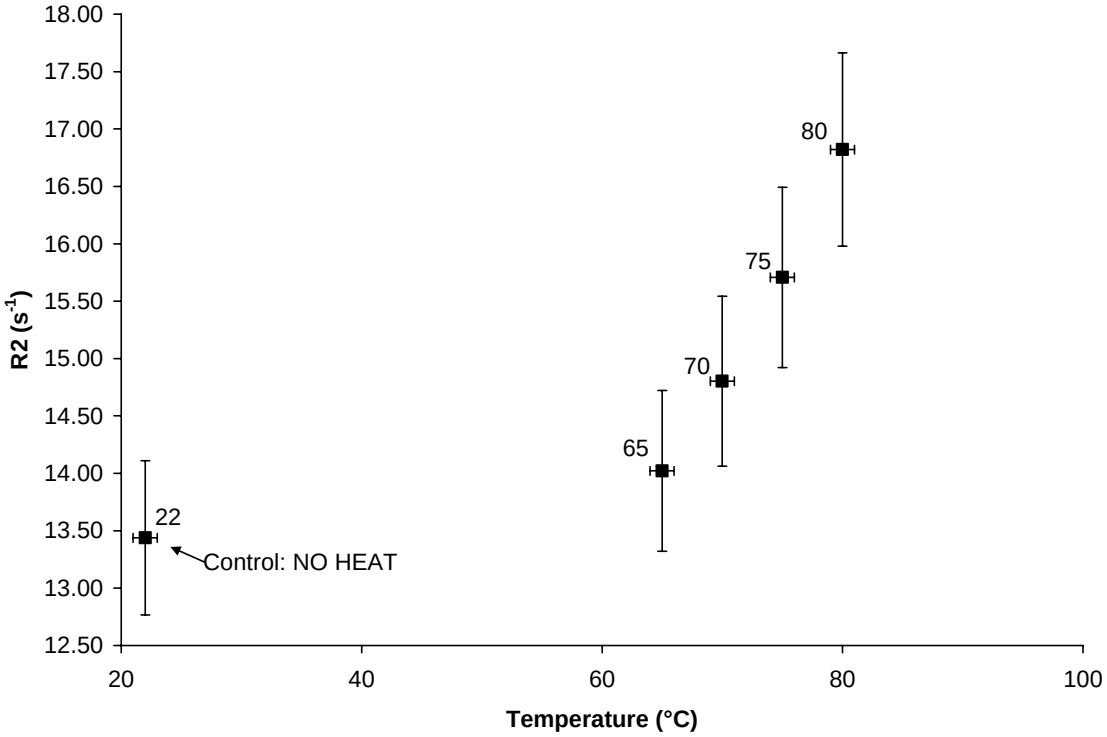

Figure 4.3: T2 relaxation rate, R2, as a function of temperature for TG1 gel.

From Figure 4.3, it is clear that TG1 is heat sensitive to temperatures in the thermal therapy regime (60 - 80 °C). TG1 gel has demonstrated unambiguous digital response capable of distinguishing temperature of at least 70 °C relative to the control sample. Additionally, focusing only in the thermal therapy temperature regime (60 – 80 °C), TG1 gel produces high degree of linearity (R^2 = 0.9935), shown in Figure 4.4. This linearity and predictable response give TG1 gel a potential to act as thermal dosimeter in therapy applications, even though this gel system is not optically tissue equivalent at NIR light regime.

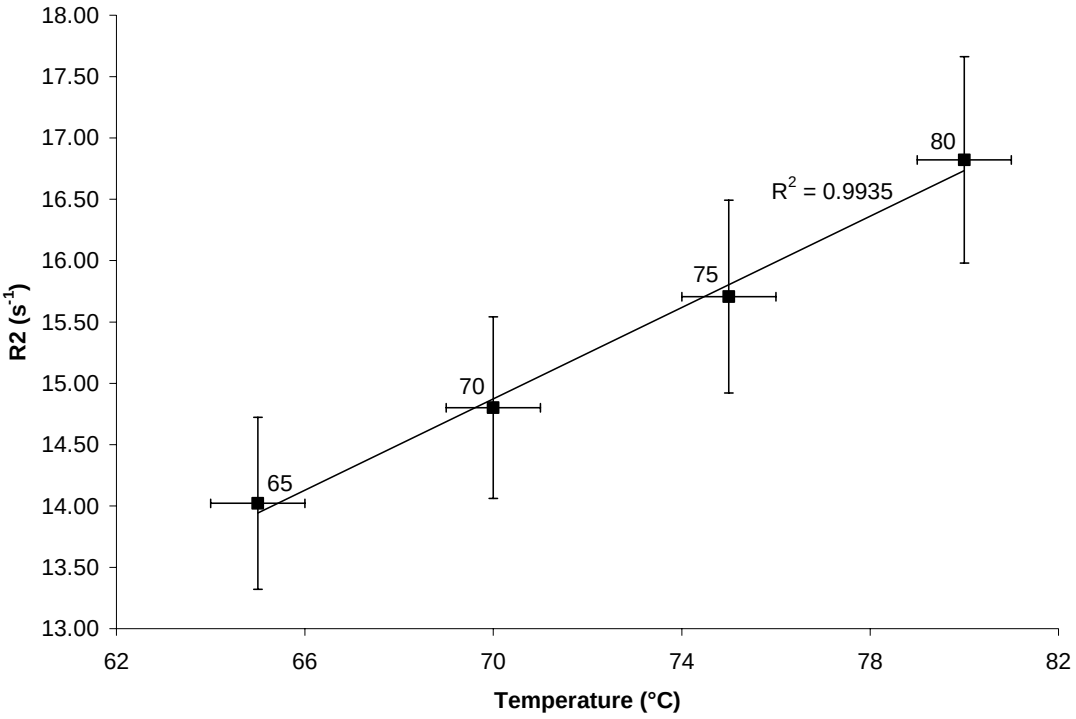

Figure 4.4: TG1 thermal response across only thermal therapy temperature regime.

The thermal response of proposed TG2, agar based gel containing BSA and Intralipid, is also characterized. Similar to TG1, TG2 gels were heated in a water bath to temperatures corresponding to thermal therapy regimes, 65-80 °C in 5 degree increments. The gels were heated to target temperature (±1 °C) and held for 2 minutes before being removed. Unlike TG1, there is no noticeable visual change in appearance with increasing temperature for TG2 gels, as shown in Figure 4.5. This lack of apparent visual change can be explained by noticing the addition of Intralipid. Intralipid, which is essentially a fat suspension, has milky-white color that masks all BSA protein denaturing resulting from heat. Consequently, MRI or optical CT must be used to thermally characterize the proposed TG2 gel.

Figure 4.5: Physical appearance of TG2 gel in response to increasing temperature.

Figure 4.6 shows the axial MRI images of TG2 gels from middle of the container. Based on Figure 4.6, there is no noticeable difference in contrast from the control sample (no heat) and that of other samples receiving heat, except for 80 °C TG2 gel sample. Table 4.3 lists the average T2 values measured for each of the five TG2 samples and their corresponding uncertainty to establish quantitative relationship. The average uncertainty in T2 values for all five samples is 3.02%.

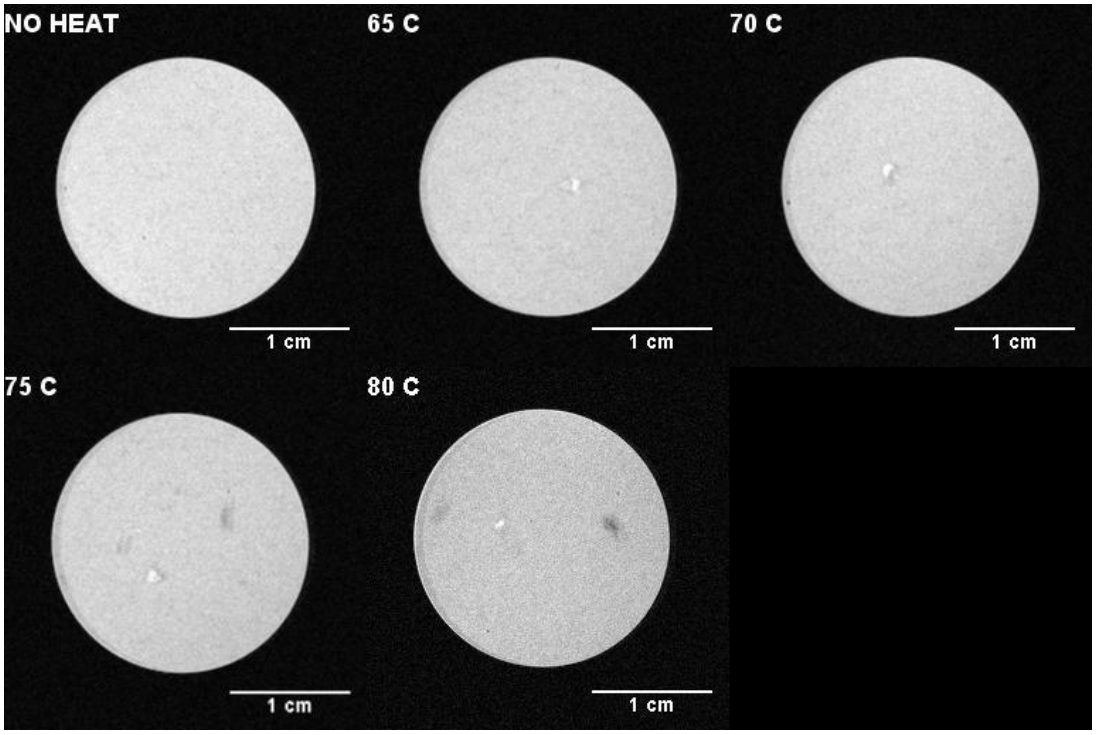

Figure 4.6: MRI images of TG2 gel samples.

Table 4.3: T2 values measured for TG2 gels as a function of temperature.

	T2 (msec)	Error (%)
No Heat (22 ± 1 °C)	57.003	2.63
65 ± 1 °C	54.093	2.76
70 ± 1 °C	56.624	2.48
75 ± 1 °C	54.305	2.94
80 ± 1 °C	48.008	4.28

Figure 4.7 shows the T2 relaxation rate, R2, for TG2 gels. From Figure 4.7, it is evident that TG2 gel is less sensitive to heat than TG1 gel. TG2 gel can only distinguish unambiguously when the temperature reaches 80 °C, based on T2 values. This digital response is less sensitive considering the fact that BSA starts to undergo denaturing at approximately 70 °C.

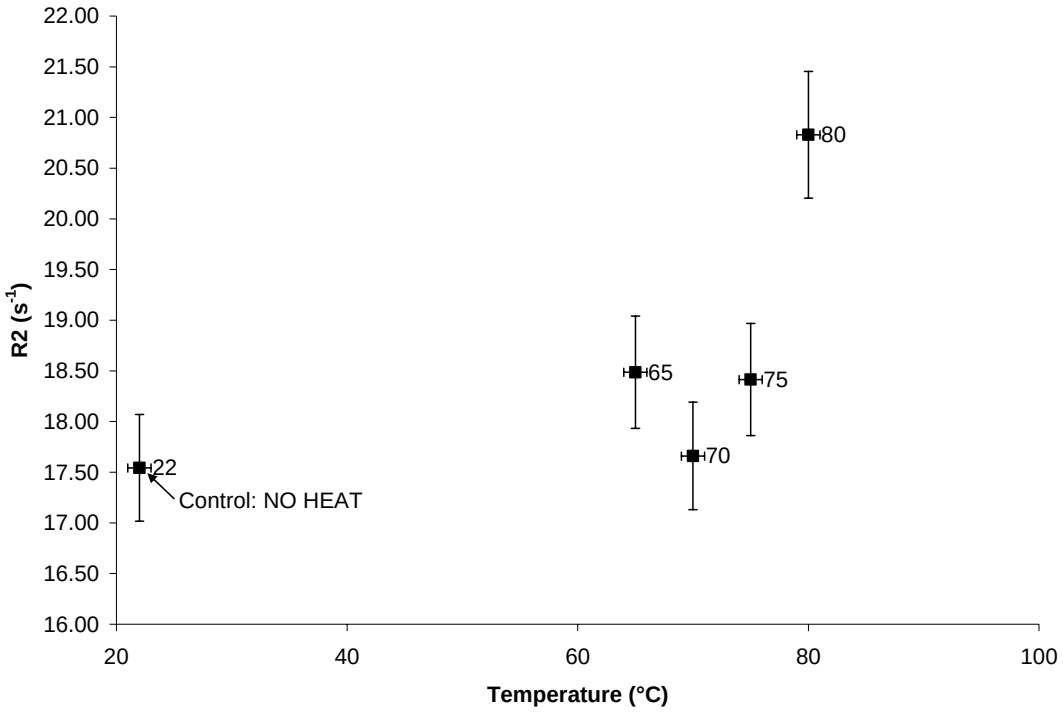

Figure 4.7: T2 relaxation rate, R2, as a function of temperature for TG2 gel.

TG2 gel is able to distinguish only 80 °C despite the fact that the heat sensitive component in TG2, BSA, begins to coagulate when the temperature exceeds 70 °C. Again, this can be explained by noticing the addition of Intralipid, which buries the signal from protein coagulation in background. However, TG2 is nonetheless shown to be heat sensitive capable of producing digital response when the temperature exceeds 80 °C. It is important to note that none of the proposed gel phantoms, TG1 and TG2, were heated above 80 °C since agar has a melting temperature range of 85-90 °C.

To summarize, two novel agar based gels are characterized in terms of their optical response to 808 nm NIR laser and their heat sensitivity. TG1 gel, agar and BSA mixture, is not optically equivalent to the previously reported gelatin based gel phantom [5]. However, TG1 gel has demonstrated unambiguous digital response capable of distinguishing temperature of at least 70 °C relative to the control sample. Additionally, focusing only in the thermal therapy temperature regime (60 – 80 °C), TG1 gel produces high degree of linearity (R^2 = 0.9935), shown in Figure 4.4. This linearity and predictable response give TG1 gel a potential to be used as thermal dosimeter in thermal therapy applications. On the other hand, TG2 has exhibited tissue equivalency based on laser transmission measurements with 808 nm NIR laser. From Figure 4.7, it is evident that TG2 gel is less sensitive to heat than TG1 gel. TG2 gel can demonstrate the heat damage unambiguously based on T2 values, only when the temperature reaches 80 °C. This digital response is considered less sensitive considering the fact that BSA starts to undergo denaturing and cause optical density change at approximately 70 °C.

CHAPTER 5

CONCLUSIONS

Two agar based non-toxic heat-sensitive gels have been developed and characterized in terms of their optical response to 808 nm NIR laser and thermal damage. Although laser transmission measurements of the gels do not yield specific quantities of μ_s' (reduced scattering coefficient) and μ_a (absorption coefficient), the obtained values essentially give an effective attenuation coefficient (μ_{eff}) of each gel taking both absorption and scattering into consideration. TG1 gel has shown to be incomparable to biological tissue based on optical transmission measurements. According to the current investigation, quantification of heat damage in the gels using average T2 values can be an acceptable method of characterization. TG1 gel has demonstrated unambiguous digital response capable of distinguishing temperature of at least 70 °C relative to the control sample. Additionally, there is a strong linear response from 65 -80 °C for TG1 with an average uncertainty of 5.03%.

The addition of Intralipid in TG2 is responsible for TG2 gel being optically tissue-equivalent for 808 nm NIR laser. Intralipid is a strong scattering media with little influence on other physical properties such as melting point. However, there is a tradeoff that is observed between tissue equivalency and heat-sensitivity for TG2. It is evident that TG2 gel is less sensitive to heat than TG1 gel because TG2 gel can exhibit the thermal damage unambiguously based on measured T2 values, only when the temperature reaches 80 °C. This digital response is considered less sensitive considering the fact that BSA starts to undergo denaturing and cause optical density change at approximately 70 °C. Unlike TG1, there is no linear response shown by TG2 with increasing temperature. Intralipid was added to establish tissue equivalency, however, the addition of Intralipid suppresses the signal from protein coagulation, thereby decreasing the heat-sensitivity of TG2 gel.

Both gels, however, have shown to be thermally stable at temperatures up to 80 °C with no evidence of gel melting being observed. The gels can be easily prepared with basic laboratory equipment, making them viable for clinical environment. Additionally, the ability of these gels to be quickly scanned under MRI is an attractive incentive for clinical applications.

CHAPTER 6

FUTURE WORK

In order to fully characterize the proposed gels, one has to determine the discrete values of μ_s' (reduced scattering coefficient) and μ_a (absorption coefficient) for each gel and how it corresponds to literature value of various tissue types. This can be done with time-resolved transmittance measurements. Additionally, the recipes proposed for both gels can be optimized in terms of their BSA and Intralipid content to enhance contrast and heat-sensitivity. Future efforts will focus on determining the optimum quantities that can be added to agar base for even higher thermal sensitivity. Besides, an alternative to Intralipid, such as food coloring or equivalent scattering media can be investigated to achieve tissue equivalency for 808 nm NIR laser.

Another critical parameter to be optimized is choice of particular heat-sensitive agent. The current work uses BSA which has a threshold temperature of 70 °C for visualization of thermal damage. Incorporation of protein or other heat-sensitive agent with much lower coagulation temperature can greatly extend the operating range of proposed gels.

Future work will also focus on development of breast phantom made of the gels developed from the current investigation. This phantom can be used for verification of diagnostic and therapeutic applications for breast cancer currently being developed based on the principles of photothermal effect with optically-tunable gold nanoparticles. During the illumination of NIR laser, heat generation within the phantom will be captured either by heat-sensitive gel itself or by thermocouples, allowing the construction of an iso-thermal map useful for therapy and detection purposes.

REFERENCES

[1] American Cancer Society. "*Cancer Facts & Figures 2008*." Atlanta: American Cancer Society; 2008. http://www.cancer.org (Accessed April 1, 2009)

[2] McDonald, M., Lochhead, S., Chopra, R., Bronskill, M. "Multi-modality tissue-mimicking phantom for thermal therapy," Phys. Med. Biol., 49, pp. 2767-2778, 2004.

[3] Fong, P. M., Keil, D. C., Does, M., Gore, J. "Polymer gels for magnetic resonance imaging of radiation dose distributions at normal room atmosphere," Phys. Med. Biol., 46, pp. 3105-3113, 2001.

[4] Iizuka, M. N., Sherar, M., Vitkin, I. "Optical phantom materials for near infrared laser photocoagulation studies," Lasers in Surgery and Medicine, 25, pp. 159-169, 1999.

[5] Chen, Y., Bailey, C., Cowan, T., Wu, F., Liu, H., Towner, R., Chen, W. "Gel phantom in selective laser phototherapy," Proc. of SPIE, vol. 6870, pp. 687008-1 – 687008-9, 2008.

[6] Terazima, M., Hirota, N., Braslavsky, S., Mandelis, A., Bialkowski, S., Diebold, G., Miller, J., Fournier, S., Palmer, R., Tam, A. "Quantities, terminology, and symbols in photothermal and related spectroscopies (IUPAC Recommendations 2004)," Pure Appl. Chem., 25, vol. 76, 6, pp. 1083-1118, 2004.

[7] Gobin, A. M., Lee, M., Halas, N., James, W., Drezek, R., West, J. "Near-infrared resonant nanoshells for combined optical imaging and photothermal cancer therapy," Nano Letters, vol. 7, 7, pp. 1929-1934, 2007.

[8] Chin, L. C., Whelan, W., Sherar, M., Vitkin, I. "Changes in relative light fluence measured during laser heating: implications for optical monitoring and modeling of interstitial laser photocoagulation," Phys. Med. Biol., 46, pp. 2407-2420, 2001.

[9] Cubeddu, R., Pifferi, A., Taroni, P., Torricelli, A., Valentini, G. "A solid tissue phantom for photon migration studies," Phys. Med. Biol., 42, pp. 1971-1979, 1997.

[10] Srinivasan R., Kumar, D., Singh, M. "Optical tissue-equivalent phantoms for medical imaging," Trends Biomater. Artif. Organs, vol. 15, 2, pp. 42-47, 2002.

[11] Weishaupt, D., Kochli, V., Marincek, B., *How does MRI work? An introduction to the physics and function of Magnetic Resonance Imaging*, Springer-Verlag, Berlin 2006.

[12] Webb, A., *Introduction to Biomedical Imaging*, Wiley-Interscience, John Wiley & Sons, New Jersey, 2003.

[13] Detector/Amplifier Hybrids with Feedback Resistor SD 112-43-11-221 http://www.advancedphotonix.com/ap_products/pdfs/SD112-43-11-221.pdf (Accessed April 5, 2009).